RSC Advances

PAPER

View Article Online
View Journal | View Issue

Check for updates

Cite this: *RSC Adv.*, 2020, **10**, 20338

Properties and mechanism for selective adsorption of Au(III) on an ionic liquid adsorbent by grafting *N*-methyl imidazole onto chloromethylated polystyrene beads†

Xin Kou, Bowen Ma, Rui Zhang, Miaomiao Cai, Yong Huang and Ying Yang *

To recover Au(III) from an acidic chloride-containing solution efficiently, an ionic liquid absorbent (CMPS-IL) was synthesized by grafting *N*-methyl imidazole onto chloromethylated polystyrene beads (CMPS). The adsorption capacity, selectivity, and reusability were systematically evaluated by a series of adsorption experiments. The maximum adsorption capacity reached up to 516.5 mg g^{-1} at 318 K. The adsorbent can selectively recover Au(III) from binary system solutions with a higher separation factor $\beta_{Au/M}$ (10^4–10^6). Moreover, the adsorption–desorption cycles (7 cycles) showed that the CMPS-IL maintained a stable adsorption performance and high adsorption efficiency. Finally, the adsorption mechanism of CMPS-IL for Au(III) was investigated by SEM, TEM, XPS, and FT-IR, then proposed with a combination of electrostatic interactions and d–π interaction between imidazolium and $AuCl_4^-$. This study provides an easily-prepared and economical adsorbent for Au(III) with high selectivity and large adsorption capacity to boost its practical applications.

Received 19th April 2020
Accepted 17th May 2020

DOI: 10.1039/d0ra03504a

rsc.li/rsc-advances

Open Access Article. Published on 27 May 2020. Downloaded on 12/10/2025 1:11:06 AM.
This article is licensed under a Creative Commons Attribution-NonCommercial 3.0 Unported Licence.

1. Introduction

In the 21st century, the age of electronic information, gold plays an increasingly significant part in many fields, especially for electrical and electronic equipment. The electronics industry consumed about 300 t of gold a year (246 t in 2009 due to worldwide economic adversity).[1] With gold concentrations in Waste Electrical and Electronic Equipment (WEEE) estimated to be 25–350 times that of primary sources (1–10 g per ton Au)[2,3] (*i.e.*, 300–350 g t^{-1} for mobile phone handsets[4] and 250 g t^{-1} for the printed circuit board of a PC[5]), WEEE is regarded as an important secondary gold resource. Processes for secondary gold production often involve refinery processes in which the gold ions must be recovered from acid leaching solutions.[6] WEEE also contains various base metals (Cu (20%), Fe (8%), Sn (4%), Ni (2%), Pb (2%), Al (2%) and Zn (1%)) that will go into leaching solutions together.[7] This inspired research into selective adsorption aiming in developing low-cost adsorbents which could recover Au(III) from complex solution.

Ion-exchange and adsorption are among the most suitable refinery methods, especially for low concentration of gold existed solutions in the practical industrial process.[8] The field of metal separation with ionic liquids-materials is a booming one and a number of studies have demonstrated that ionic liquids-materials represented high adsorption capacities for metal seperation.[9–15] A lot of typical carriers for IL, such as metal organic frameworks (MOFs),[16] nanomaterials[17,18] (nano-silica, nanospheres, nanotubes, nanowire), biopolymers,[19,20] and traditional polymers[21] are reported in recent years. An ionic liquid modified MOF sorbent was synthesized and used for removal of chromium ion from aqueous media by A. Nasrollahpour.[16] The sorption was maximum for the initial pH of 2.0 at 285.71 mg g^{-1}. Mohamed E. Mahmoud[17] has reported supported hydrophobic ionic liquid on nano-silica for adsorption of lead which had excellent metal capacity values toward Pb(II) sorption, extraction and removal of Pb(II) from strongly acidic as well as other aqueous solutions (pH 1–7). Dong *et al.*[19] has synthesized a series of imidazolium-based ionic liquid modifying cellulose microsphere as Au(III) adsorbents and confirmed that ion exchange certainly occurred during adsorption by XPS analysis. In 2018, our group[21] synthesized a *N*-methylimidazolium-based poly(ionic liquid) with maximum adsorption capacity of 158.774 mg g^{-1} for Au(III). As competitive alternatives, MOFs, nano materials, and biopolymers have been certified to be promising carriers. Nevertheless, the high cost of them does not make it possible for large-scale industrial applications. Moreover, the size of adsorbents should also be considered, which related to the filtration properties of adsorbents. In any case, a facile, low-cost, and user-friendly approach to achieve high-efficiency

The Key Laboratory of Nonferrous Metals Chemistry and Resources Utilization of Gansu Province, School of Chemistry and Chemical Engineering, Lanzhou University, Lanzhou 730000, P. R. China. E-mail: yangying@lzu.edu.cn

† Electronic supplementary information (ESI) available. See DOI: 10.1039/d0ra03504a

This journal is © The Royal Society of Chemistry 2020

Open Access Article. Published on 27 May 2020. Downloaded on 12/10/2025 1:11:06 AM.
This article is licensed under a Creative Commons Attribution-NonCommercial 3.0 Unported Licence.

adsorption for valuable metals with excellent selectivity is a crucial but unsettled issue.

Inspired by the previous work, mesoporous cross-linked chloro-methylated polystyrene (CMPS) beads, which is a widely employed macromolecular support of thermal stability and economic applicability to continuous processes,[22] were used as a support to prepare an absorbent with high adsorption capacity, high selectivity, and low cost in present work. The effects of the dosage of CMPS-IL, pH value and disturbing ions on the recovery of Au(III) were systematically studied. The thermodynamics and kinetics of adsorption were carried out in detail. The adsorption mechanism was further investigated by SEM, TEM, FT-IR, and XPS.

2. Experimental

2.1 Reagents and materials

Cross-linked chloro-methylated polystyrene (CMPS) beads (0.7–1 mm) were bought from Energy Chemical Reagent Co., Ltd. Dissolving 1 g of gold in aqua regia prepared initial aqueous solutions of $HAuCl_4$ which tested by atomic absorption spectroscopy (AAS). A solution of 50 mg L^{-1} Au(III) was prepared after dilution of the initial aqueous solution. The binary ion stock solutions were prepared by dissolving metal chlorides in distilled water: $FeCl_3 \cdot 6H_2O$, $NiCl_2 \cdot 6H_2O$, $CoCl_2 \cdot 6H_2O$, $2CdCl_2 \cdot 5H_2O$, and $CuCl_2 \cdot 2H_2O$. All the other reagents were of analytical reagent grade.

2.2 Synthesis of the CMPS-IL

2.48 g (30.2 mmol) of *N*-methyl imidazole and 10 g of CMPS beads were refluxed with 4.60 g of KOH as catalysts in 180 mL of acetonitrile at 70 °C for 72 h. The solid products were filtered and repeatedly rinsed with distilled water to neutral at room temperature. Then the products were dried in vacuum at 35 °C for three days and the dark yellow beads (CMPS-IL) were obtained. The preparation route was described in Scheme 1.

2.3 Batch adsorption studies

40 mg of CMPS-IL and 50 mL of Au(III) solutions (50 mg L^{-1}) were applied to extraction experiments in sealed conical flasks. Experiments of adsorption isotherm were proceeded at the Au(III) concentration range from 50–2800 mg L^{-1} 0.1 mol L^{-1} HCl or 0.1 mol L^{-1} NaOH was used to tune the pH value. For the adsorption kinetic texts, CMPS-IL (120 mg) and Au(III) solution (50 mg L^{-1}, 150 mL) were shaking for a specified time (5–180 min) at pH level of 2.0. 1 g L^{-1} of Fe(III), Cu(II), Co(II), Ni(II) and Cd(II) were chosen as the competitive metal ions to investigate the selectivity of CMPS-IL.

The recovery percentage (%) and adsorption amount q_e (mg g^{-1}) were obtained as follows:

$$\text{Recovery } (\%) = \frac{C_0 - C_e}{C_0} \times 100 \quad (1)$$

$$q_e = \frac{(C_0 - C_e)}{m} \times V \quad (2)$$

where C_0 and C_e (mg L^{-1}) represent the initial and equilibrium concentrations of Au(III); V (L) is the volume of the aqueous phase; m (g) is the dose of CMPS-IL.

The separation factor ($\beta_{Au/M}$) can be calculated from the following equations:

$$\beta_{Au/M} = \frac{Q_{e,Au}}{C_{e,Au}} \Big/ \frac{Q_{e,M}}{C_{e,M}} \quad (3)$$

where Q_e is the amount of metal adsorbed at equilibrium per unit weight of adsorbent (mmol g^{-1}); C_e is the equilibrium concentration of metal ions in solution (mmol L^{-1}).

2.4 Characterization

Elemental analysis of C, N and H was performed on a VarioEL elemental analyzer. FT-IR measurement was recorded on a NEXUS 670 spectrometer using KBr. SEM images were taken with a field-emission scanning electron microscope (JEOLJSM-6701F). Metal ion solution (Au(III), Fe(III), Cu(II), Ni(II), Cd(II), and Co(II)) were determined by AAS (AA240, Edinburgh Instruments; flame: acetylene and air; flow rate: air-10 L min^{-1}, acetylene-1 L min^{-1}; wavelength: Au-242.8 nm; Fe-248.7 nm; Cu-324.8 nm; Ni-352.5 nm; Cd-228.8 nm; Co-240.7 nm). DSC curves were obtained by differential scanning calorimeter (NETZSCH200F3). Thermogravimetric (TGA) tests were conducted on a Shimadzu TG 60 thermogravimetric analyzer under a N_2 dynamic atmosphere (50 cm^3 min^{-1}) in the temperature range of 25–800 °C, with a heating rate of 10 °C min^{-1}. X-ray photoelectron spectroscopy (XPS) measurements were recorded on an AXIS Ultra X-ray photoelectron spectrometer (Kratos Analytical-A Shimadzu Group Company, Japan), using monochromatic Al-Kα radiation as the excitation and choosing C 1s (284.6 eV) as the reference (Kratos, UK). The morphologies of symbols were carried out by means of a field-emission scanning electron microscope (Fe-SEM, NOVA NanoSEM 450). Scanning transmission electron microscope (TEM) images were obtained using Tecnai F30 transmission electron microscope (Philips-

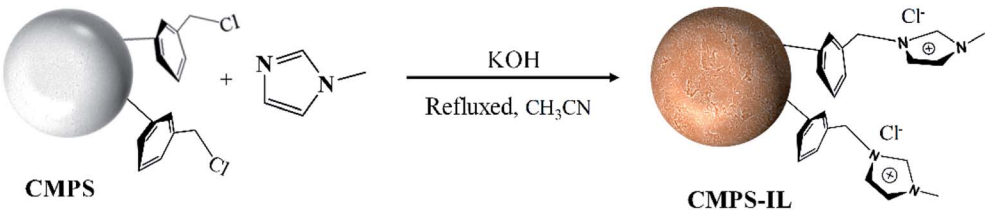

Scheme 1 Preparation route of the CMPS-IL.

Open Access Article. Published on 27 May 2020. Downloaded on 12/10/2025 1:11:06 AM.
This article is licensed under a Creative Commons Attribution-NonCommercial 3.0 Unported Licence.

FEI, Holland). The surface area (S_{BET}) was estimated by Brunauer–Emmett–Teller (BET) method. The total pore volumes (V_{total}) were evaluated from the liquid volume of N_2 at a relative pressure (p/p_0) of 0.99.

3. Results and discussion

3.1 Preparation and characterization of the CMPS and CMPS-IL

Fig. 1(a) showed the FT-IR spectra of CMPS, CMPS-IL and Au(III) loaded CMPS-IL. Compared with the original CMPS beads, the characteristic absorption bands of C–Cl at 668 cm^{-1} and 1263 cm^{-1} disappeared,[23] and there emerged some new characteristic adsorption bands for CMPS-IL. Evidence of the presence of the imidazole group was that characteristic imidazole ring peaks existing at 1577 cm^{-1} (imidazole ring bending), 1387 cm^{-1} and 1347 cm^{-1} (N–C/C–C stretching), 1158 cm^{-1} (in-plane ring C–H bending).[24]

The N_2 adsorption–desorption isotherms were used to investigate specific surface area and porous structures of the CMPS and CMPS-IL in Fig. 1(c) and (d). The BET surface areas of CMPS and CMPS-IL were 60.39 $m^2\ g^{-1}$ and 4.86 $m^2\ g^{-1}$; pore volume also became smaller than that before modification (0.35 $cm^3\ g^{-1}$ and 0.02 $cm^3\ g^{-1}$), which might be caused by the introduction and hydration of imidazole.[25] As shown in Fig. 1(b), the CMPS-IL samples experienced a weight loss of less than 7% in the temperature range from 80 to 150 °C, which supported complete dehydration. TGA curves in Fig. 1(b) showed that CMPS-IL was stable below 200 °C.

3.2 Extraction studies

3.2.1 Effects of initial pH and CMPS-IL dosage on adsorption. The removal rate of Au(III) at different pH values (1.0–6.0) at 25 °C was presented in Fig. 2(a). The extraction efficiency was not too different when the pH was varied from 1.0 to 3.0 (98.74–99.23%). The adsorption efficiency sharply decreased over the pH range 4.0–6.0, which was by reason of the formation of chloride–hydroxide complexes of Au(III) and the competition between OH^- and $AuCl_4^-/AuCl_3(OH)^-$.[26,27] Considering a practical application scene, the pH value was chosen at 1.0 and it was used in the following experiments. The effect of CMPS-IL dosage (range 0.3–0.9 g L^{-1}) on adsorption of gold was shown in Fig. 2(b). The result concluded that the CMPS-IL dosage of 0.8 g L^{-1} was suitable for 50 mg L^{-1} of Au(III).

3.2.2 Adsorption kinetics. Fig. 3(a) presented the adsorption kinetic data at different temperature, representing that

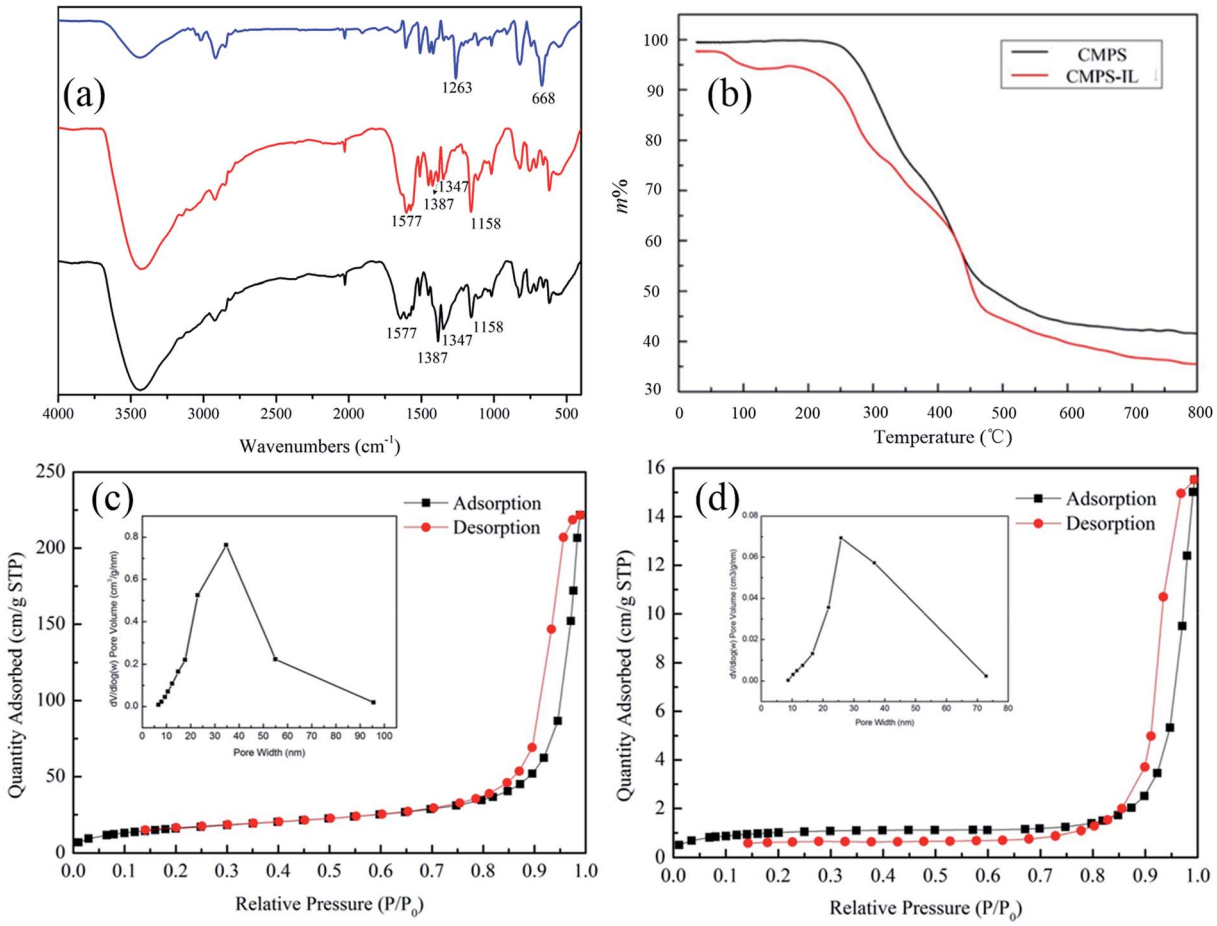

Fig. 1 (a) The FT-IR spectra of CMPS (blue), CMPS-IL (red) and Au(III) loaded CMPS-IL (black); (b) TGA curves of CMPS and CMPS-IL; (c and d): N_2 adsorption–desorption isotherm and pore size distributions of CMPS and CMPS-IL.

 This journal is © The Royal Society of Chemistry 2020

Open Access Article. Published on 27 May 2020. Downloaded on 12/10/2025 1:11:06 AM.
This article is licensed under a Creative Commons Attribution-NonCommercial 3.0 Unported Licence.

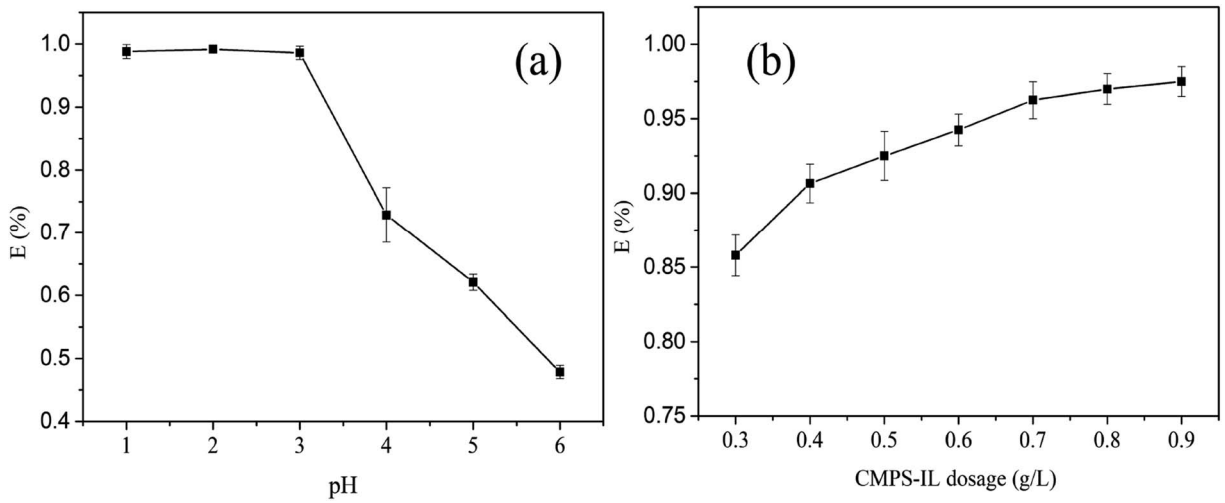

Fig. 2 Influencing factors of extraction efficiency of Au(III): (a) pH; (b) CMPS-IL dosage.

adsorption capacity increased as contact time increased. Within the first hour, Au(III) was rapidly adsorbed on the surface of CMPS-IL, and the adsorption amount reached 51.4 mg g^{-1} (298 K). Then the adsorption rate gradually slowed down, when the adsorption amount reached 57.1 mg g^{-1} (298 K) at 2 h, the amount of adsorption was no longer increasing, reaching equilibrium adsorption capacity. It can be clearly seen that higher temperature favors CMPS-IL adsorption of Au(III).

The adsorption kinetic data was investigated with pseudo-first-order (eqn (4)) and pseudo-second-order (eqn (5)) as follows:

$$\ln(q_e - q_t) = \ln q_e - k_1 t \quad (4)$$

$$\frac{t}{q_t} = \frac{1}{k_2 q_e^2} + \frac{t}{q_e} \quad (5)$$

where q_e (mg g^{-1}) and q_t (mg g^{-1}) represents the extraction capacities of Au(III) at equilibrium and time t (h), respectively. k_1 is the first-order rate constant at equilibrium (h^{-1}). k_2 is the second-order rate constant at equilibrium (g (mg h)$^{-1}$).

Table S2† summarized the kinetic parameters at different temperatures. The higher R^2 showed that the pseudo-second-order model was more suitable to describe the kinetic process suggesting that chemisorption had the stronger influence on the adsorption of the Au(III).[28] In addition, the experimental data of the extraction capacities were 58.71 mg g^{-1}, 60.92 mg g^{-1} and 65.98 mg g^{-1} corresponding to 298 K, 308 K and 318 K, which were closed to the calculated values of 64.52 mg g^{-1}, 66.27 mg g^{-1} and 71.33 mg g^{-1} based on the pseudo-second-order model. According to Fig. 3(c), even though the linear correlation between square root of time and q_e was good, the plots did not pass through the origin, which indicated that intraparticle diffusion may be involved in the adsorption process but it may not be the controlling factor in determining the kinetics of the process.[29]

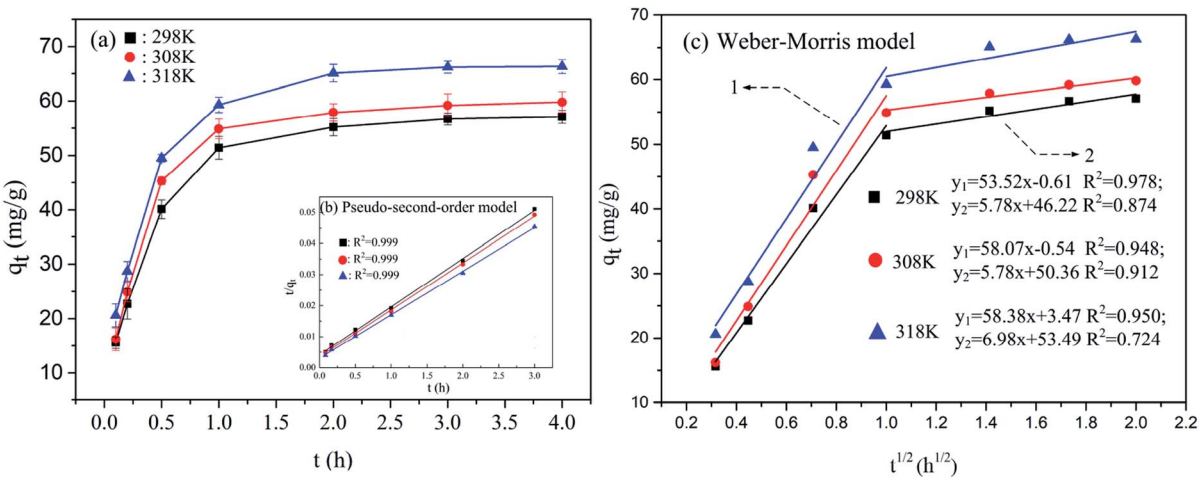

Fig. 3 (a) Adsorption kinetics of CMPS-IL for Au(III) at different temperatures; (b) pseudo-second-order model for Au(III) adsorption; (c) Weber–Morris model.

Open Access Article. Published on 27 May 2020. Downloaded on 12/10/2025 1:11:06 AM.
This article is licensed under a Creative Commons Attribution-NonCommercial 3.0 Unported Licence.

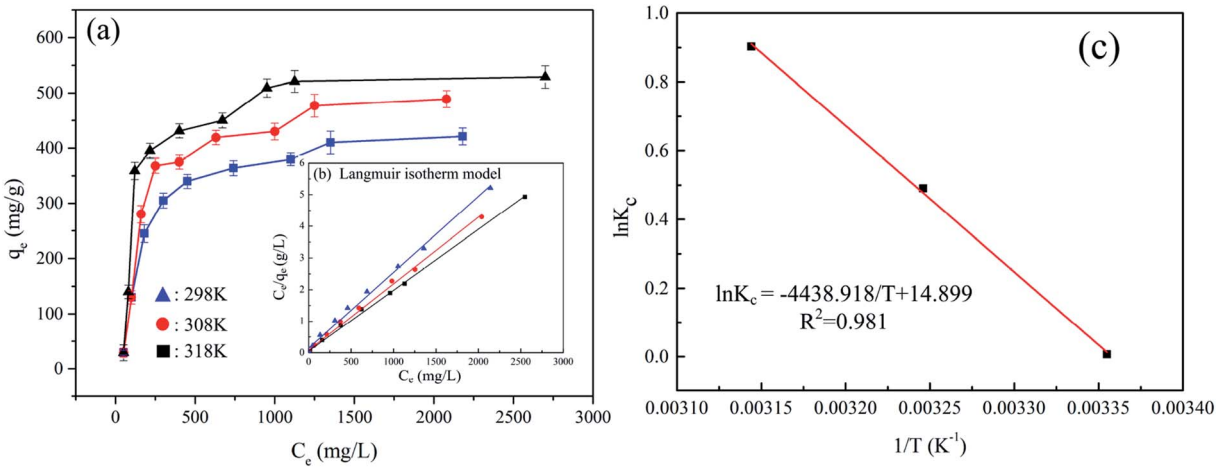

Fig. 4 (a) Adsorption isotherms of CMPS-IL towards Au(III); (b) Langmuir isotherms of Au(III) adsorption on CMPS-IL; (c) plot of ln K_c *vs.* 1/T based Van't Hoff relation.

3.2.3 Adsorption isotherms. The adsorption isotherm indicates the relationship between the equilibrium concentration of the $AuCl_4^-$ in the solution at the equilibrium of adsorption and how the adsorption capacity varies with the adsorption concentration. The curves of initial Au(III) concentration and adsorption amount at different temperature were shown in Fig. 4(a) to ascertain the maximum adsorption capacity of Au(III). Langmuir isotherm and Freundlich isotherm were the commonest used isotherms to match the experimental values. The models can be expressed as eqn (6) and (7).

Langmuir isotherm linear equation:[30]

$$\frac{C}{q_e} = \frac{1}{q_{max}b} + \frac{C_e}{q_{max}} \quad (6)$$

Freundlich isotherm linear equation:[31]

$$\ln\ q_e = \ln\ K_f + \frac{1}{n}\ln\ C_e \quad (7)$$

where C_e (mg L^{-1}) is the equilibrium concentration of Au(III), q_e (mg g^{-1}) is the equilibrium extraction capacity, q_{max} is the maximum adsorption capacity, and b is the adsorption equilibrium constant related to the adsorption energy for Langmuir isotherm model. K_f and n are Freundlich isotherm constants.

The corresponding adsorption parameters, along with correlation coefficients, were listed in Table S3.† The maximum extraction capacity for Au(III) was estimated to be 516.5 mg g^{-1} at 318 K. According to the higher correlation coefficient (R^2 = 0.994 at 298 K, R^2 = 0.996 at 308 K, R^2 = 0.998 at 318 K), the Langmuir adsorption isotherm which assumes that ideal adsorption occurs with each adsorption site binding one adsorbate molecule then forming a monolayer adsorption was fit better with the experimental data. Therefore, the mechanism of the adsorption of Au(III) by CMPS-IL is presumed monolayer adsorption and chemisorption and without interaction between adsorbed species. Dimensionless separation factor (R_L) which is used to measure favorability of adsorption, was calculated using eqn (8).

$$R_L = \frac{1}{1 + bC_0} \quad (8)$$

where C_0 is the initial metal concentration (mg L^{-1}) and b is the Langmuir parameter. The conditions $R_L > 1$: unfavorable; R_L = 1: linear; $0 < R_L < 1$: favorable; and $R_L = 0$: irreversible reported in literature[32] when compared with the calculated values of R_L (0.2535–0.0107 seen in Fig. S4†) revealed that the adsorption of Au(III) on CMPS-IL was favorable and reversible.

3.2.4 Thermodynamics of Au(III) adsorption on CMPS-IL. Thermodynamics parameters can determine the feasibility and nature of the adsorption process. Gibbs free energy (ΔG), enthalpy (ΔH), and entropy (ΔS) for the Au(III) adsorption process were acquired by using the following equations:[33,34]

$$K_c = \frac{q_e}{C_e} \quad (9)$$

$$\ln\ K_c = \frac{\Delta S}{R} - \frac{\Delta H}{RT} \quad (10)$$

$$\Delta G = \Delta H - T\Delta S \quad (11)$$

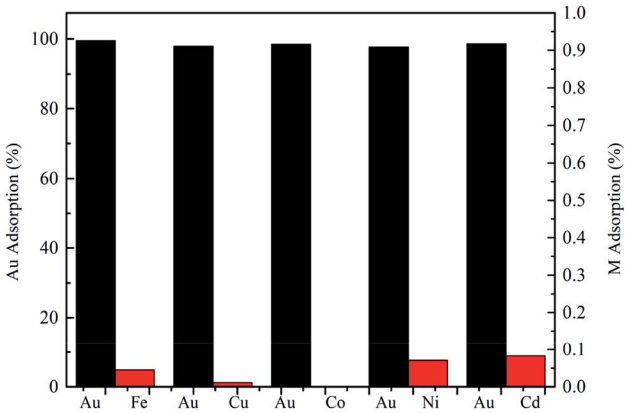

Fig. 5 Extraction behaviors of Au(III) from binary ion systems.

This journal is © The Royal Society of Chemistry 2020

Open Access Article. Published on 27 May 2020. Downloaded on 12/10/2025 1:11:06 AM.
This article is licensed under a Creative Commons Attribution-NonCommercial 3.0 Unported Licence.

where R, T and K_c are the gas constant (8.314 J mol^{-1} K^{-1}), absolute temperature (K) and the thermodynamics constant, respectively.

The enthalpy and entropy values were calculated from the slope and intercept of the plot of ln K_c *vs.* $1/T$.[35] The calculated thermodynamic parameters were listed in Table S3.† ΔG (kJ mol^{-1}) (298 K, −0.002; 308 K, −1.239; 318 K, −2.476) is negative and the absolute value increases with the increase of temperature, showing that the adsorption process is feasible and spontaneous and high temperature is beneficial to the adsorption process. The positive values of ΔH illustrated that the reaction between CMPS-IL and Au(III) was endothermic, which was also consistent with the results of adsorption kinetics.[36] The positive value of ΔS (123.7 J mol^{-1} K^{-1}) showed that the sorption of gold was correlated to an increased randomness.[37] In addition, the absolute value of $T\Delta S$ is larger than ΔH, which reveals that the adsorption of Au(III) is dominated by entropic changes rather than the enthalpic changes.[38,39]

3.2.5 Effect of diverse ions on the extraction of Au(III). Usually, there is a certain concentration of Fe(III), Cu(II), Co(II), Ni(II) and Cd(II) coexisting with Au(III) in an acid leaching solution of WEEE. The coexistence metal ions might distract with the extraction selectivity of Au(III). To further study Au(III) adsorption efficiency, interferences by coexisting ions were tested. As shown in Fig. 5, the adsorption efficiency of Au(III) was more than 95% in each binary ion system. Table S4† listed the data of the separating coefficient ($\beta_{Au/M}$) and extraction efficiency (E_{Au}), which obviously higher than many current adsorbents. As a result, the adsorbent had enormous potential to extract Au(III) selectively from acid complex solution system in the industrial process. The effect of Cl^- concentration on extraction efficiencies of Au(III) by CMPS-IL was described in Fig. 6. The recovery efficiency for the Au(III) ions was slightly decreased with increasing chloride ion concentration, however, its values were above 95%.

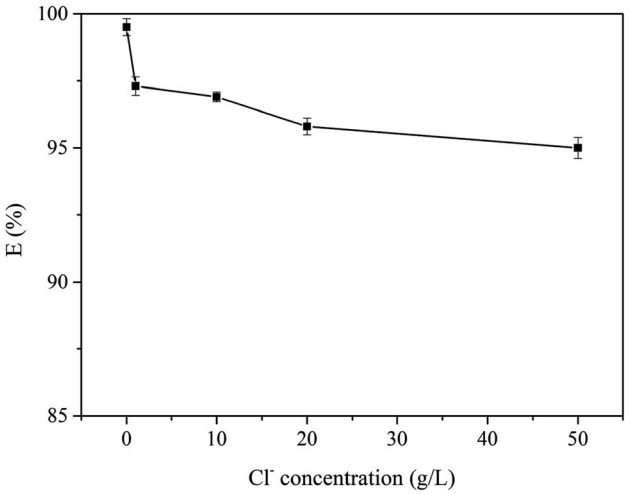

Fig. 6 The effect of chloride ion concentration on Au(III) recovery (conditions: pH = 2, T = 298 K).

Table 1 summarized Au(III) recovery on various adsorbents reported in the literature. CMPS-IL exhibited high adsorption capacity and excellent selectivity for Au(III) from mixed aqueous solution, implying that CMPS-IL was of potential application value in the practical industrial process for the extraction separation and recovery of Au(III).

3.3 Recovery of Au(III) and reusability of CMPS-IL

The reusability of CMPS-IL was significant for practical application. Au(III) saturated CMPS-IL, which was prepared as follows: 40 mg of CMPS-IL is added to 50 mL of Au(III) solution (pH 2.0 and an initial concentration of 300 mg L^{-1}), and the mixture solution is shocked for 2 h under 298 K, is subjected to adsorption/desorption cycles. It was observed in Fig. S4† that 40 mg of Au(III) saturated CMPS-IL could be easily eluted with 50 mL of the mixture of HCl–thiourea solution with a desorption ratio of 99%. Fig. 7 showed the extraction and

Table 1 Characterization of different types of absorbents (chosen examples) for adsorption of Au(III)

Types of ion exchangers	Adsorption capacity (mg g^{-1})	Selectivity towards Cu, Ni ($\beta_{Au/M}$)	Equilibrium time (h)	Synthesis method	Particle size (μm)	Reusability	References
Polyethylenimine modified speciosa leaves powder	286–313	Cu: 695 Ni: —	6	One step	200–300	7	40
Polystyrene-supported 3-amino-1,2-propanediol	300.8	10^2–10^3	12	One-step	—	—	41
Aminomethyl pyridine functionalized adsorbents based on cellulose	315–517	687–829	12	Two steps	220	—	42
Aliquat-336-impregnated alginate capsule	191.92	—	6	Three steps	3000	4	43
Cellulose microsphere with imidazolium-based ionic liquid	454–735	—	2	Two steps	200–300	—	19
D301 resin modified with containing N/S functional polymer	274–300	500–700	5	Three steps	500–700	5	44
CMPS-IL	410–516	10^4–10^5	2	One step	700–1000	7	This work

Open Access Article. Published on 27 May 2020. Downloaded on 12/10/2025 1:11:06 AM.
This article is licensed under a Creative Commons Attribution-NonCommercial 3.0 Unported Licence.

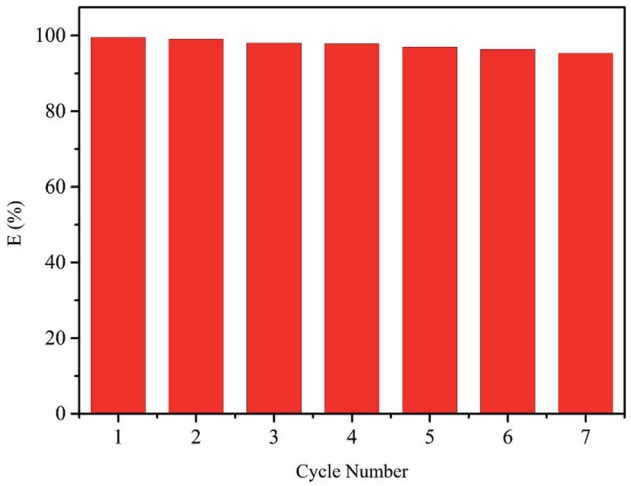

Fig. 7 Extraction and stripping cycles of CMPS-IL.

stripping studies of CMPS-IL, the recovery percentage of Au(III) was always more than 95% over 7 successive cycles, the results indicated a relatively good reusability of CMPS-IL. Ionic liquids are organic salts composed of asymmetric organic cations and organic or inorganic anions with high thermal and chemical stability and can therefore be used to recover gold from highly acidic and high concentration chloride systems.

3.4 Adsorption mechanism discussion

3.4.1 XPS analysis of CMPS-IL and Au loaded CMPS-IL. The chemical composition of CMPS-IL before and after adsorption was investigated by XPS. Au 4f XPS-peak-differentiation-imitating analyses of the spectrum were applied to evaluate the existence form of sorbed gold on CMPS-IL. The Au 4f peaks (Fig. 8(b)) could be deconvoluted into three chemical state: Au(0) at $4f_{7/2}$ 84.00 eV and $4f_{5/2}$ 87.85 eV, Au(III) with weak d–π reaction at $4f_{7/2}$ 87.39 eV and $4f_{5/2}$ 91.31 eV and Au(III) with strong d–π reaction at $4f_{7/2}$ 89.76 eV and $4f_{5/2}$ 93.39 eV.

Au(0) species were discovered in both Au salt ($KAuCl_4$: Au(0) $4f_{7/2}$ 84.00 eV, $4f_{5/2}$ 87.65 eV) in the literature[45] and sorbed gold on CMPS-IL. The Binding Energy (BE) of sorbed Au(III) was higher than that of Au salt ($KAuCl_4$)[45] summarized in Table 2, which indicated a lower electron density at the Au center in sorbed gold on CMPS-IL. That may be caused by the electrons of the Au atoms in $AuCl_4^-$ being donated to the N atoms in the imidazolium[46,47] and forming π bonding when $AuCl_4^-$ and imidazole ring were in a parallel position, which was also confirmed by single-crystal structure analysis in our last report.[21] However, due to the steric hindrance effect, part of $AuCl_4^-$ could not be in a parallel position with imidazole ring, which weakened the d–π reaction. As a result, there appeared two sets of peaks of Au(III): one was Au(III) with a weak d–π reaction and the other was Au(III) with a strong d–π reaction.

The N 1s spectra in Fig. 9(a) showed two asymmetric peaks at 401.80 and 399.31 eV. They were assigned to the N atoms in the imidazolium in ionic liquids[48,49] and free *N*-methyl imidazole impurities,[50] respectively. After gold adsorption, part of N atoms accepted electrons of the Au atoms, and BE decreased from 401.8 to 399.0. The BE of the N uninvolved reaction was unchanged, which made N ls "doublet" in Fig. 9(b).

3.4.2 Morphology and structure analysis. The morphology of CMPS-IL after adsorption Au(III) was investigated by TEM,

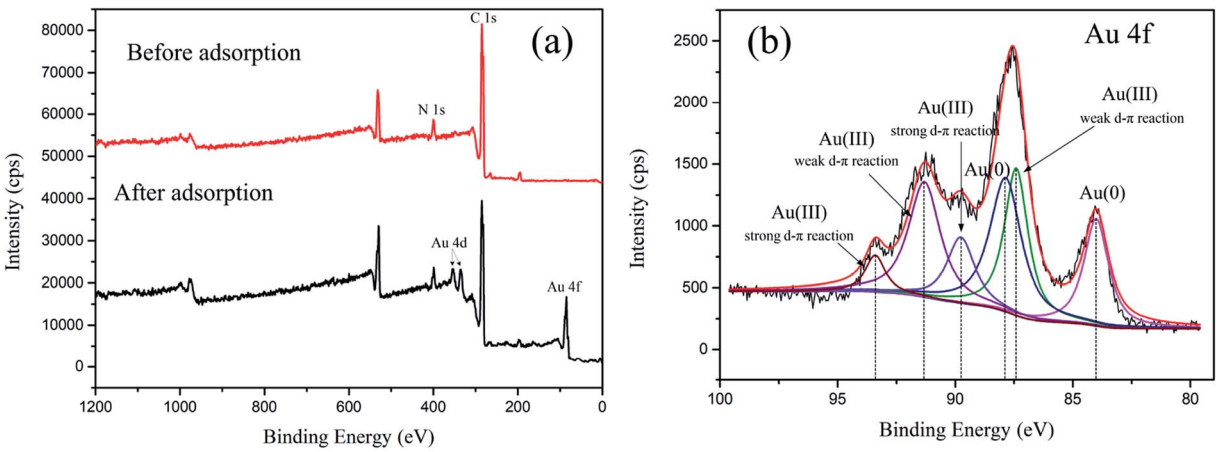

Fig. 8 (a) The XP spectra of CMPS-IL before and after adsorption, (b) the high-resolution XP spectrum of Au 4f.

Table 2 The comparison of BE of $KAuCl_4$ and sorbed gold on CMPS-IL

	Au(0)	Au(III) $4f_{7/2}$	Au(III) $4f_{5/2}$
Au salt ($KAuCl_4$)[45]	84.00	87.2 eV	90.8 eV
Sorbed Au on CMPS-IL	84.00	87.39 eV (weak d–π reaction) 89.76 eV (strong d–π reaction)	91.31 eV (weak d–π reaction) 93.39 eV (strong d–π reaction)

 This journal is © The Royal Society of Chemistry 2020

Open Access Article. Published on 27 May 2020. Downloaded on 12/10/2025 1:11:06 AM.
This article is licensed under a Creative Commons Attribution-NonCommercial 3.0 Unported Licence.

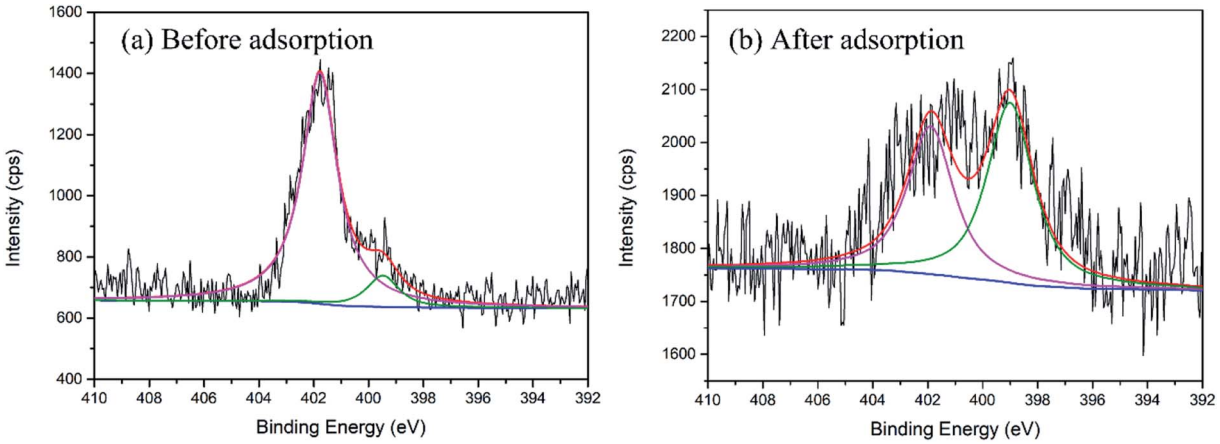

Fig. 9 The XP spectra of the N 1s in CMPS-IL (a) before and (b) after adsorption.

SEM, element mapping, and element distribution (Fig. 10). It can be observed that the surface of CMPS was smooth and had a lot of tiny cracks and pores (Fig. 10(a)). CMPS-IL owned a rough, wrinkled surface and smaller cracks and holes (Fig. 10(b)). There were several particles of different sizes distributed on the surface of the CMPS-IL after adsorption clearly (Fig. 10(c)), and element mapping results verified that stacks of Au element existed on these particles (Fig. 10(d)). In high magnification TEM images of Fig. 10(g) and (h), the lattice fringe of 0.235 nm can be observed clearly, corresponding to the *d*-spacing of the Au (111) plane,[51,52] which indicated the existence of Au (0) species.

3.4.3 Infrared analysis. Also, the extraction mechanism of CMPS-IL for Au(III) can also be proved by FT-IR spectra. The enhancement of peaks at 1387 cm^{-1} and 1347 cm^{-1} after adsorption attributed to the characteristic peak of C–C/N–C stretching in Fig. 1, which indicated an interaction between $AuCl_4^-$ and imidazolium.

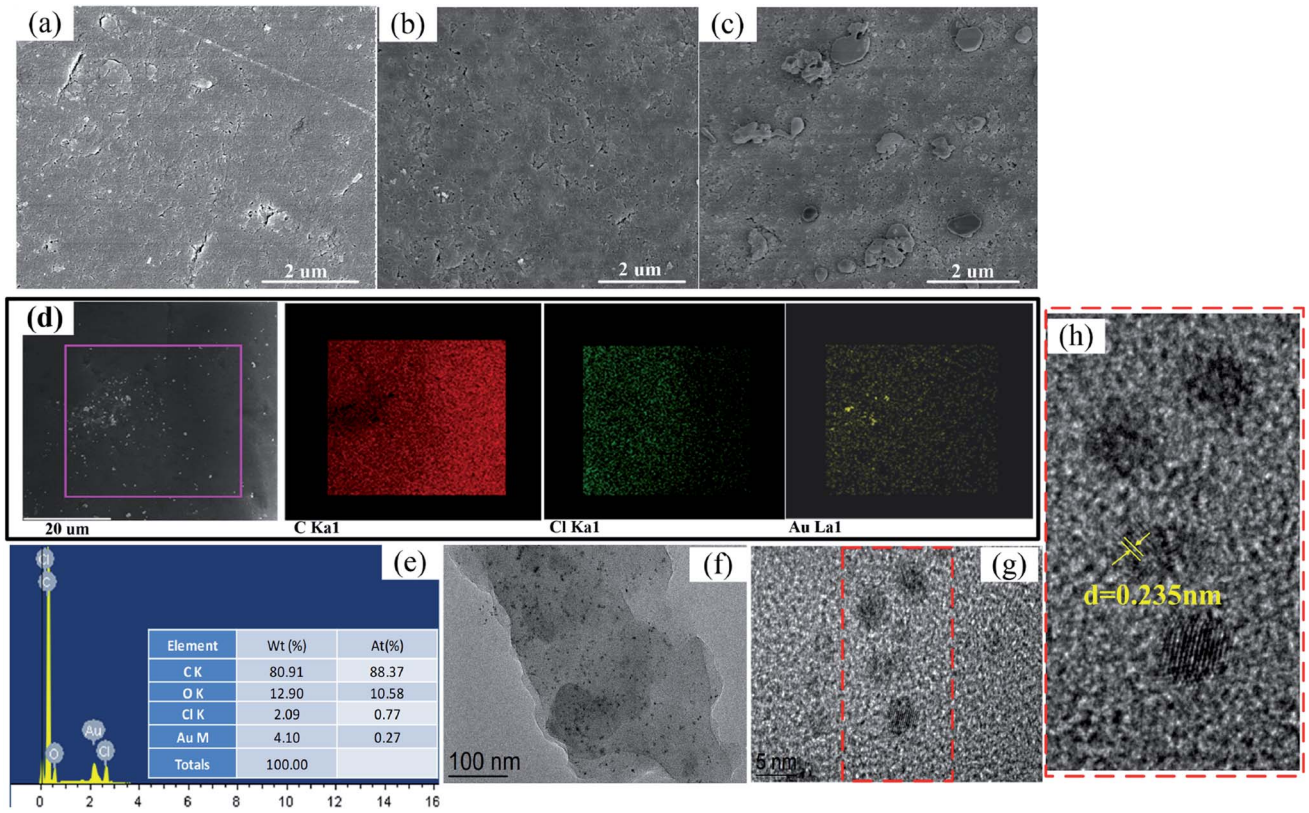

Fig. 10 The SEM images of (a) the CMPS, (b) the CMPS-IL, (c) the Au-loaded CMPS-IL. (d) Element mapping of the Au-loaded CMPS-IL, (e) EDX analyses of Au-loaded CMPS-IL. TEM images of Au-loaded CMPS-IL: (f) scale bars = 100 nm, (g) scale bars = 5 nm, (h) partial enlarged detail of (g).

Open Access Article. Published on 27 May 2020. Downloaded on 12/10/2025 1:11:06 AM.
This article is licensed under a Creative Commons Attribution-NonCommercial 3.0 Unported Licence.

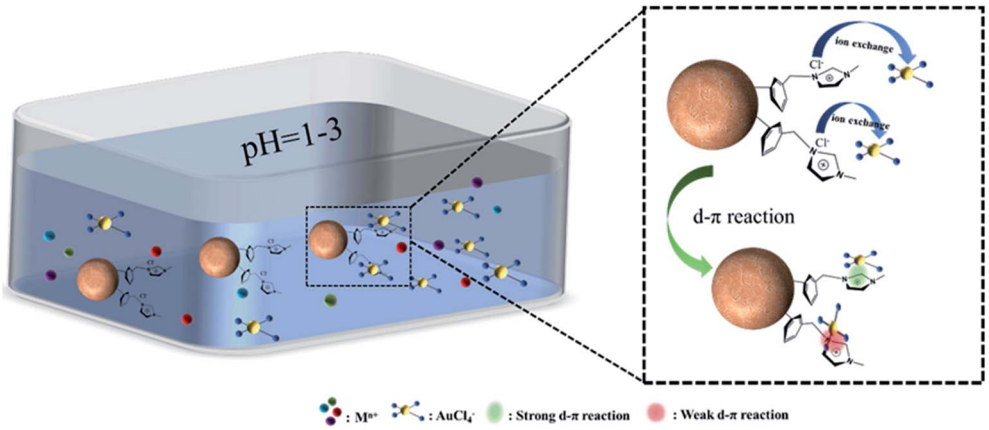

Fig. 11 The adsorption mechanism of Au(III) by CMPS-IL.

In conclusion, the mechanism of Au(III) recovery by CMPS-IL was considered a combination of electrostatic interactions, strong and weak d–π interactions between imidazolium and $AuCl_4^-$ exhibited in Fig. 11.

4. Conclusion

Our study presented a low-cost and highly selective ionic liquid adsorbent (CMPS-IL) prepared in one step by grafting *N*-methyl imidazole onto CMPS beads, which could be used for gold recovery from a complex system. The experiment results indicated the CMPS-IL has an effective extraction effect on Au(III). The Au(III) adsorption on CMPS-IL reached equilibrium within 2 h. Kinetic data suggested a pseudo-second-order kinetic model for Au(III) adsorption. The maximum monolayer adsorption capacity of Au(III) by CMPS-IL was in the range of 410.9–516.5 mg g^{-1} at 298–318 K. In the binary ion systems (Fe(III), Cu(II), Co(II), Ni(II) and Cd(II)), the CMPS-IL had an excellent selectivity for gold ($\beta = 10^4$–10^6). The XPS results suggested there were weak and strong d–π reaction between $AuCl_4^-$ and imidazolium besides electrostatic interactions. Finally, the CMPS-IL would be a promising gold absorbent for its high adsorption capacity, high selectivity, and good cycle performance.

Conflicts of interest

There are no conflicts to declare.

Acknowledgements

This work was supported by Major Science and Technology Projects by Gansu Province, China (19ZD2GC001).

References

1 GFMS Ltd, *Gold Survey 2010*, London, 2010.
2 G. M. Mudd, Global trends in gold mining: towards quantifying environmental and resource sustainability?, *Resour. Policy*, 2007, **32**, 42–56.
3 A. Tuncuk, V. Stazi, A. Akcil, E. Y. Yazici and H. Deveci, Aqueous metal recovery techniques from e-scrap: hydrometallurgy in recycling, *Miner. Eng.*, 2012, **25**, 28–37.
4 J. Cui and L. Zhang, Metallurgical recovery of metals from electronic waste: a review, *J. Hazard. Mater.*, 2008, **158**, 228–256.
5 C. Hagelüken and C. W. Corti, Recycling of gold from electronics: cost-effective use through 'Design for Recycling, *Gold Bull.*, 2010, **43**, 209–220.
6 R. Widmer, O.-K. Heidi, S.-K. Deepali, M. Schnellmann and H. Böni, Global perspectives on E-waste, *Environ. Impact Assess. Rev.*, 2005, **25**, 436–458.
7 E. Y. L. Sum, The Recovery of Metals from Electronic Scrap, *JOM*, 1991, **43**, 53–61.
8 N. V. Nguyen, J. Jeong, M. K. Jha, J. Lee and K. O. Asare, Comparative studies on the adsorption of Au (III) from waste rinse water of semiconductor industry using various resins, *Hydrometallurgy*, 2010, **105**, 161–167.
9 H. Zhang, M. Shang, C. Shen, G. Li and Y. Su, Continuous Extraction of Gold(III) Using Pyridine Ionic Liquid-Based Water-in-Oil microemulsion in microreactors, *Ind. Eng. Chem. Res.*, 2019, **58**, 12729–12740.
10 S. Katsuta, Y. Watanabe, Y. Araki and Y. Kudo, Extraction of Gold(III) from Hydrochloric Acid into Various Ionic Liquids: Relationship between Extraction Efficiency and Aqueous Solubility of Ionic Liquids, *ACS Sustainable Chem. Eng.*, 2016, **4**, 564–571.
11 N. Papaiconomou, G. Vite, N. s. Goujon, J. M. Lévêquea and I. Billard, Efficient removal of gold complexes from water by precipitation or liquid-liquid extraction using ionic liquids, *Green Chem.*, 2012, **14**, 2050–2056.
12 Y. Tong, H. Yang, J. Li and Y. Yang, Extraction of Au (III) by ionic liquid from hydrochloric acid medium, *Sep. Purif. Technol.*, 2013, **120**, 367–372.
13 Y. Zheng, Y. Tong, S. Wang, H. Zhang and Y. Yang, Mechanism of gold (III) extraction using a novel ionic liquid-based aqueous two phase system without additional extractants, *Sep. Purif. Technol.*, 2015, **154**, 123–127.
14 V. T. Nguyen, J. Lee, J. Jeong, B.-S. Kim, G. Cote and A. Chagnes, Extraction of Gold(III) from Acidic Chloride

 This journal is © The Royal Society of Chemistry 2020

Open Access Article. Published on 27 May 2020. Downloaded on 12/10/2025 1:11:06 AM.
This article is licensed under a Creative Commons Attribution-NonCommercial 3.0 Unported Licence.

Media Using Phosphonium-based Ionic Liquid as an Anion Exchanger, *Ind. Eng. Chem. Res.*, 2015, **54**, 1350–1358.

15 L. Mark, Ionic Liquids as Extraction Solvents: Where do We Stand?, *Sep. Sci. Technol.*, 2006, **41**, 2047–2063.

16 A. Nasrollahpour and S. E. Moradi, Hexavalent chromium removal from water by ionic liquid modified metal-organic frameworks adsorbent, *Microporous Mesoporous Mater.*, 2017, **243**, 47–55.

17 M. E. Mahmouda and H. M. Al-Bishri, Supported hydrophobic ionic liquid on nano-silica for adsorption of lead, *Chem. Eng. J.*, 2011, **166**, 157–167.

18 Y. Ai, M. Wu, L. Li, F. Zhao and B. Zeng, Highly selective and effective solid phase microextraction of benzoic acid esters using ionic liquid functionalized multiwalled carbon nanotubes-doped polyaniline coating, *J. Chromatogr. A*, 2016, **1437**, 1–7.

19 Z. Dong and L. Zhao, Surface modification of cellulose microsphere with imidazolium-based ionic liquid as adsorbent: effect of anion variation on adsorption ability towards Au (III), *Cellulose*, 2018, **25**, 2205–2216.

20 X. Sun, B. Peng, Y. Ji, J. Chen and D. Li, Chitosan(Chitin)/Cellulose Composite Biosorbents Prepared Using Ionic Liquid for Heavy Metal Ions Adsorption, *AIChE J.*, 2009, **8**(55), 2062–2069.

21 Z. Xu, Y. Zhao, W. Liang, P. Zhou and Y. Yang, A novel N-methylimidazolium-based poly(ionic liquid) to recover trace tetrachloroaurate from aqueous solution based on multiple supramolecular interactions, *Inorg. Chem. Front.*, 2018, **5**, 922–931.

22 Y. Liu, Z. Zhang, P. Wang and Y. Dong, Surface charge modification of chloromethylated polystyrene beads with NaH for the removal of sulfamonomethoxine, *J. Taiwan Inst. Chem. Eng.*, 2016, **65**, 22–27.

23 Y. Zhang, Y. Chen, C. Wang and Y. Wei, Immobilization of 5-aminopyridine-2-tetrazole on cross-linked polystyrene for the preparation of a new adsorbent to remove heavy metal ions from aqueous solution, *J. Hazard. Mater.*, 2014, **276**, 129–137.

24 D. W. O'Connell, B. A. C. Birkinshaw, T. F. O'Dwyer and T. F. O'Dwyer, A study of the mechanisms of divalent copper binding to a modified cellulose adsorbent, *J. Appl. Polym. Sci.*, 2010, **116**, 2496–2503.

25 P. I. Nagy, G. J. Durant and D. A. Smith, Theoretical studies on hydration of pyrrole, imidazole, and protonated imidazole in the gas phase and aqueous solution, *J. Am. Chem. Soc.*, 1993, **115**, 2912–2922.

26 P. J Murphy and M. S. LaGrange, Raman spectroscopy of gold chloro-hydroxy speciation in fluids at ambient temperature and pressure: a re-evaluation of the effects of pH and chloride concentration, *Geochim. Cosmochim. Acta*, 1998, **62**, 3515–3526.

27 A. Aydin, M. Ímamoğlu and M. Gülfen, Separation and recovery of gold(III) from base metal ions using melamine-formaldehyde-thiourea chelating resin, *J. Appl. Polym. Sci.*, 2008, **107**, 1201–1206.

28 M. K. Amosa, Sorption of water alkalinity and hardness from high-strength wastewater on bifunctional activated carbon: process optimization, kinetics and equilibrium studies, *Environ. Technol.*, 2016, **37**, 2016–2039.

29 M. Zhao, J. Zhao, Z. Huang, S. Wang and L. Zhang, One pot preparation of magnetic chitosan-cystamine composites for selective recovery of Au(III) from the aqueous solution, *Int. J. Biol. Macromol.*, 2019, **137**, 721–731.

30 I. Langmuir, The Constitution and Fundamental Properties of Solids and Liquids. Part II. Liquids, *J. Am. Chem. Soc.*, 1917, **39**, 1848–1906.

31 L. P. Lingamdinne, Y. Y. Chang, J. K. Yang, J. Singh, E. H. Choi and M. Shiratani, Biogenic reductive preparation of magnetic inverse spinel iron oxide nanoparticles for the adsorption removal of heavy metals, *Chem. Eng. J.*, 2017, **307**, 74–84.

32 H. Gao, Y. Wang and L. Zheng, Hydroxyl-functionalized ionic liquid-based cross-linked polymer as highly efficient adsorbent for anionic azo dyes removal, *Chem. Eng. J.*, 2013, **234**, 372–379.

33 A. Maleki, B. Hayati, F. Najafi, F. Gharibi and S. W. Joo, Heavy metal adsorption from industrial wastewater by PAMAM/TiO_2 nanohybrid: preparation, characterization and adsorption studies, *J. Mol. Liq.*, 2016, **224**, 95–104.

34 T. A. Saleh, A. Sari and M. Tuzen, Effective adsorption of antimony(III) from aqueous solutions by polyamide-graphene composite as a novel adsorbent, *Chem. Eng. J.*, 2017, **307**, 230–238.

35 M. Can, E. Bulut and M. Özacarb, Reduction of palladium onto pyrogallol-derived nano-resin and its mechanism, *Chem. Eng. J.*, 2015, **275**, 322–330.

36 A. D. Dwivedi, S. P. Dubey, S. Hokkanen, R. N. Fallah and M. Sillanpää, Recovery of gold from aqueous solutions by taurine modified cellulose: an adsorptive-reduction pathway, *Chem. Eng. J.*, 2014, **255**, 97–106.

37 B. C. Choudhary, D. Paul, A. U. Borse and D. J. Garole, Surface functionalized biomass for adsorption and recovery of gold from electronic scrap and refinery wastewater, *Sep. Purif. Technol.*, 2018, **195**, 260–270.

38 N. You, X.-F. Wang, J.-Y. Li, H.-T. Fan, H. Shen and Q. Zhang, Synergistic removal of arsanilic acid using adsorption and magnetic separation technique based on Fe_3O_4@graphene nanocomposite, *J. Ind. Eng. Chem.*, 2019, **70**, 346–354.

39 X. Gao, J. Liu, M. Li, C. Guo, H. Long, Y. Zhang and L. Xin, Mechanistic study of selective adsorption and reduction of Au (III) to gold nanoparticles by ion-imprinted porous alginate microspheres, *Chem. Eng. J.*, 2019, **385**, 123897.

40 B. C. Choudhary, D. Paul, A. U. Borse and D. J. Garole, Surface functionalized biomass for adsorption and recovery of gold from electronic scrap and refinery wastewater, *Sep. Purif. Technol.*, 2018, **195**, 260–270.

41 C. Sun, G. Zhang, C. Wang, R. Qu, Y. Zhang and Q. Gu, A resin with high adsorption selectivity for Au (III): Preparation, characterization and adsorption properties, *Chem. Eng. J.*, 2011, **172**, 713–720.

42 Z. Dong, J. Liu, W. Yuana, Y. Yi and L. Zhao, Recovery of Au(III) by radiation synthesized aminomethyl pyridine functionalized adsorbents based on cellulose, *Chem. Eng. J.*, 2016, **283**, 504–513.

Open Access Article. Published on 27 May 2020. Downloaded on 12/10/2025 1:11:06 AM.
This article is licensed under a Creative Commons Attribution-NonCommercial 3.0 Unported Licence.

43 W. Wei, D. H. K. Reddy, J. K. Bediako and Y. Yun, Aliquat-336-impregnated alginate capsule as a green sorbent for selective recovery of gold from metal mixtures, *Chem. Eng. J.*, 2016, **289**, 413–422.

44 F.-Q. An, M. Li, X.-D. Guo, H.-Y. Wang, R.-Y. Wu, T.-P. Hu, J. Gao and W.-Z. Jiao, Selective adsorption of $AuCl_4^-$ on chemically modified D301 resin with containing N/S functional polymer, *J. Environ. Chem. Eng.*, 2017, **5**, 10–15.

45 D. W. Hatchett, M. Josowicz, J. Janata and D. R. Baer, Electrochemical Formation of Au Clusters in Polyaniline, *Chem. Mater.*, 1999, **11**, 2989–2994.

46 R. D. Feltham and P. Brant, XPS Studies of Core Binding Energies in Transition Metal Complexes. 2. Ligand Group Shifts, *J. Am. Chem. Soc.*, 1982, **104**, 641–645.

47 T. M. Ivanova, R. V. Linko, A. V. Petrov, M. I. Bazanov and K. M. Dyumaev, Effect of the Nature of Axial Ligand on the Effective Charge of the Metal Center in PcFe(II) Complexes, *Russ. J. Inorg. Chem.*, 2008, **53**, 1784–1787.

48 M. V. Zeller and R. G. Hayes, X-Ray Photoelectron Spectroscopic Studies on the Electronic Structures of Porphyrin and Phthalocyanine Compounds, *J. Am. Chem. Soc.*, 1973, **95**, 3855–3860.

49 C. F. Vernon, P. D. Fawell and C. Klauber, XPS investigation of the states of adsorption of aurocyanide onto crosslinked polydiallylamine and commercial anion-exchange resins, *React. Polym.*, 1992, **18**, 35–45.

50 J. E. Pereira da Silva, D. L. A. de Faria, S. I. Córdoba de Torresi and M. L. A. Temperini, Influence of Thermal Treatment on Doped Polyaniline Studied by Resonance Raman Spectroscopy, *Macromolecules*, 2000, **33**, 3077–3083.

51 A. Nazirov, A. Pestov, Y. Privar, A. Ustinov, E. Modin and S. Bratskaya, One-pot green synthesis of luminescent gold nanoparticles using imidazole derivative of chitosan, *Carbohydr. Polym.*, 2016, **151**, 649–655.

52 Y. Su, X. Li, Y. Wang, H. Zhong and R. Wang, Gold nanoparticles supported by imidazolium-based porous organic polymers for nitroarene reduction, *Dalton Trans.*, 2016, **45**, 16896–16903.

 This journal is © The Royal Society of Chemistry 2020